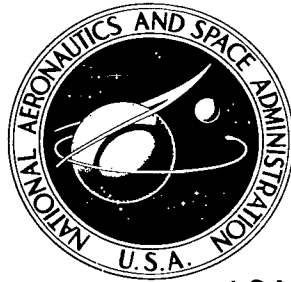


NASA TECHNICAL NOTE



NASA TN D-5484

2.1

LOAN COPY: RETURN  
AFWL (WDL-2)  
KIRTLAND AFB, N M

1512510



NASA TN D-5484

CAVITATION DAMAGE AND THE  
EFFECT OF FLUID TEMPERATURE  
ON THE PERFORMANCE OF AN  
AXIAL-FLOW PUMP IN LIQUID SODIUM

by Walter S. Cunnan and Dean C. Reemsnyder

Lewis Research Center  
Cleveland, Ohio



0132151

1. Report No. NASA TN D-5484	2. Government Accession No.	3. Recipient's Catalog No.	
4. Title and Subtitle <b>CAVITATION DAMAGE AND THE EFFECT OF FLUID TEMPERATURE ON THE PERFORMANCE OF AN AXIAL-FLOW PUMP IN LIQUID SODIUM</b>		5. Report Date October 1969	6. Performing Organization Code
7. Author(s) Walter S. Cunnan and Dean C. Reemsnyder	8. Performing Organization Report No. E-4942		
9. Performing Organization Name and Address Lewis Research Center National Aeronautics and Space Administration Cleveland, Ohio 44135	10. Work Unit No. 720-03		
12. Sponsoring Agency Name and Address National Aeronautics and Space Administration Washington, D.C. 20546	11. Contract or Grant No.		
	13. Type of Report and Period Covered Technical Note		
15. Supplementary Notes	14. Sponsoring Agency Code		
16. Abstract <p>An axial-flow pump with three different blade materials was tested for 232 hours in liquid sodium at temperatures of 1000° and 1500° F (811 and 1089 K). Noncavitation performance is essentially independent of fluid temperature in this range. A maximum reduction in required net positive suction head of 13 feet (4 m) under that at 1000° F (811 K) was obtained in 1500° F (1089 K) sodium. The reduction increased with increasing flow coefficient, increasing rotative speed, and decreasing head-rise-coefficient ratio. Severe suction-surface cavitation damage occurred near the blade-tip leading edges after a 32-hour cavitation damage test. Rene' 41 is more resistant to cavitation damage from sodium than either the 316 or 318 stainless-steel blades. And cavitation damage increases significantly with rotative speed at constant suction specific speed.</p>			
17. Key Words (Suggested by Author(s)) Cavitation damage in sodium Liquid-metal pump Axial-flow sodium pump Pump blade materials in sodium	18. Distribution Statement Unclassified - unlimited		
19. Security Classif. (of this report) Unclassified	20. Security Classif. (of this page) Unclassified	21. No. of Pages 25	22. Price* \$3.00

\*For sale by the Clearinghouse for Federal Scientific and Technical Information  
Springfield, Virginia 22151

# CAVITATION DAMAGE AND THE EFFECT OF FLUID TEMPERATURE ON THE PERFORMANCE OF AN AXIAL-FLOW PUMP IN LIQUID SODIUM

by Walter S. Cunnan and Dean C. Reemsnyder

Lewis Research Center

## SUMMARY

An axial-flow rotor with three different blade materials was tested for 232 hours in liquid sodium at temperatures of  $1000^{\circ}$  and  $1500^{\circ}$  F (811 and 1089 K). The 5-inch (127-mm) research rotor had nine insertable double-circular-arc blades of three different materials, a blade-tip diffusion factor of 0.40, a hub-tip radius ratio of 0.77, and a blade-tip solidity of 1.0. After noncavitating and cavitating performance was obtained, a 32-hour cavitation test was conducted in  $1500^{\circ}$  F (1089 K) sodium at 7200 rpm and at a suction specific speed of about 6100.

Pump noncavitating performance is essentially independent of fluid temperature to  $1500^{\circ}$  F (1089 K). An inflection of the head-flow characteristic curve occurs near the design flow coefficient. Cavitating performance indicates that initial head-rise dropoff occurs at a suction specific speed of about 5500. This modest suction capability is attributed to the low blade-tip solidity of 1.0 and the high hub-tip radius ratio of 0.77. These were dictated by the requirement of insertable blades and the system flow characteristics, respectively.

A reduction in required net positive suction head was measured in  $1500^{\circ}$  F (1089 K) liquid sodium under that at  $1000^{\circ}$  F (811 K). The reduction increased from a very slight value at the lowest flow coefficient to about 13 feet (4 m) at 7200 rpm and at the highest flow coefficient of 0.173. This reduction increases with increasing flow coefficient, increasing rotative speed, and decreasing head-rise-coefficient ratio. Similar trends for the effect of fluid temperature on cavitation performance were obtained for a similar rotor in water at temperatures to  $250^{\circ}$  F (394 K).

The rotor blades sustained severe localized suction-surface cavitation damage near the blade-tip leading edges. The three Rene' 41 (a nickel-chromium-based superalloy) blades sustained less cavitation damage than either the 316 or 318 stainless-steel blades. This cavitation damage was more severe than that sustained in an earlier test by a similar rotor in  $1500^{\circ}$  F (1089 K) sodium during a longer endurance test (200 hr) at the same suction specific speed but a lower rotative speed (3450 rpm). Thus, the intensity of cavitation damage increases significantly with rotative speed and cannot be predicted by suction specific speed alone.

## INTRODUCTION

In space power systems utilizing the Rankine cycle with liquid alkali metals as the working fluid, the condensate pump must operate with high-temperature liquid metals near saturation conditions. Thus, cavitation is a serious problem; it can cause a decrease in pump performance and can result in damage to the pump blading.

In a previous investigation (ref. 1), a 5-inch (127-mm) axial-flow rotor was tested for 558 hours in sodium at temperatures to  $1500^{\circ}$  F (1089 K). That rotor, as well as the one used in the present investigation, had nine insertable blades, three each of Rene' 41, 316 stainless steel, and 318 stainless steel. A 200-hour cavitation endurance test was conducted at 3450 rpm in  $1500^{\circ}$  F (1089 K) liquid sodium and at a suction specific speed of about 6500. The rotor sustained light cavitation damage near the tip leading edge of the blades. The nickel-chromium-based superalloy (Rene' 41) blades were more resistant to cavitation damage from high-temperature sodium than either the 316 or 318 stainless-steel blades.

In order to observe the type of cavitation formations which probably occurred in the rotor in liquid sodium, a similar axial-flow rotor was tested in deaerated water at temperatures to  $250^{\circ}$  F (394 K) (ref. 2). The rotors had identical hydrodynamic and blade designs except for opposite directions of rotation. Visual and photographic observations indicated that initial head-rise dropoff occurred when the tip vortex cavitation over the middle third of the blade chord covered the outer third of the flow passage. No difference in cavitation performance was detected in water between  $80^{\circ}$  and  $175^{\circ}$  F (300 and 352 K). Cavitation performance in  $250^{\circ}$  F (394 K) water improved significantly over that for room-temperature water. At similar operating conditions, a reduction in the required net positive suction head of 2 to 6 feet (0.6 to 1.8 m) under that required at  $80^{\circ}$  F (300 K) was measured at a pump inlet temperature of  $250^{\circ}$  F (394 K). The improvement in cavitation performance increased with increasing flow coefficient and with decreasing head-rise-coefficient ratio.

This investigation was conducted to determine the effect of fluid temperature on the cavitation performance of the pump operated in liquid sodium. Another objective was to evaluate qualitatively the effect of increased rotative speed on the intensity of cavitation damage at a constant suction specific speed. The relative resistance to cavitation damage of three blade materials in high-temperature liquid sodium are compared with the results of reference 1. A rotor identical to that of reference 1 and with the same three blade materials has been tested in liquid sodium at temperatures of  $1000^{\circ}$  and  $1500^{\circ}$  F (811 and 1089 K). Operating test conditions were varied over a range of rotative speeds from 3500 to 7200 rpm, flow coefficients from 0.11 to 0.18, and net positive suction heads from 25 to 175 feet (7.6 to 53.3 m).

## APPARATUS AND PROCEDURE

The axial-flow rotor, pump assembly, test facility, and instrumentation used in this investigation are essentially the same as that described in detail in reference 1. Only a brief discussion is presented herein.

### Pump Rotor Design and Description

The axial-flow rotor is shown in figure 1. The rotor is 5 inches (127 mm) in diameter.

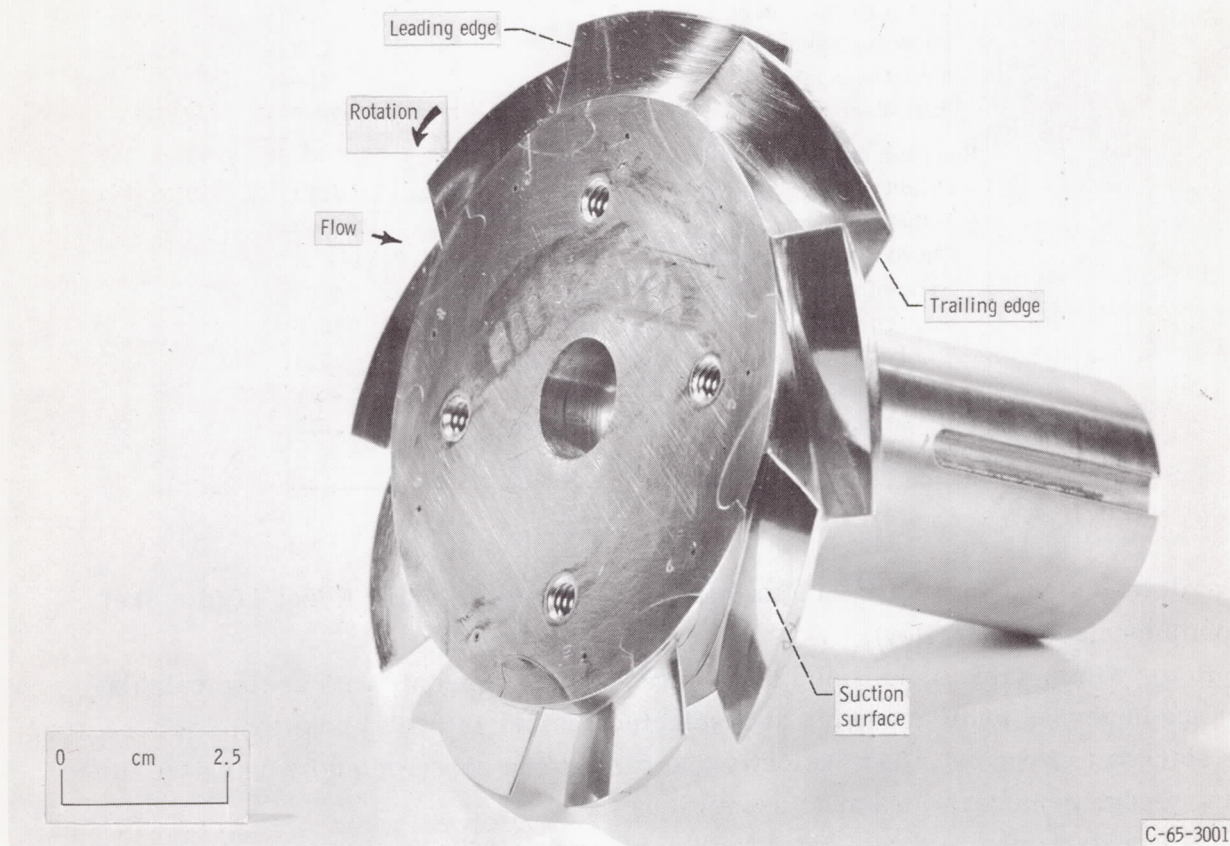


Figure 1. - Axial-flow rotor before test.

ter with a hub-tip radius ratio of 0.77. Principal blade-design parameters are listed in table I. The rotor consists of nine double-circular-arc blades in close-fitting slots in the hub. The insertable blades were secured with rollpins. Three of the blades are

TABLE I. - BLADE DESIGN PARAMETERS OF  
AXIAL-FLOW ROTOR

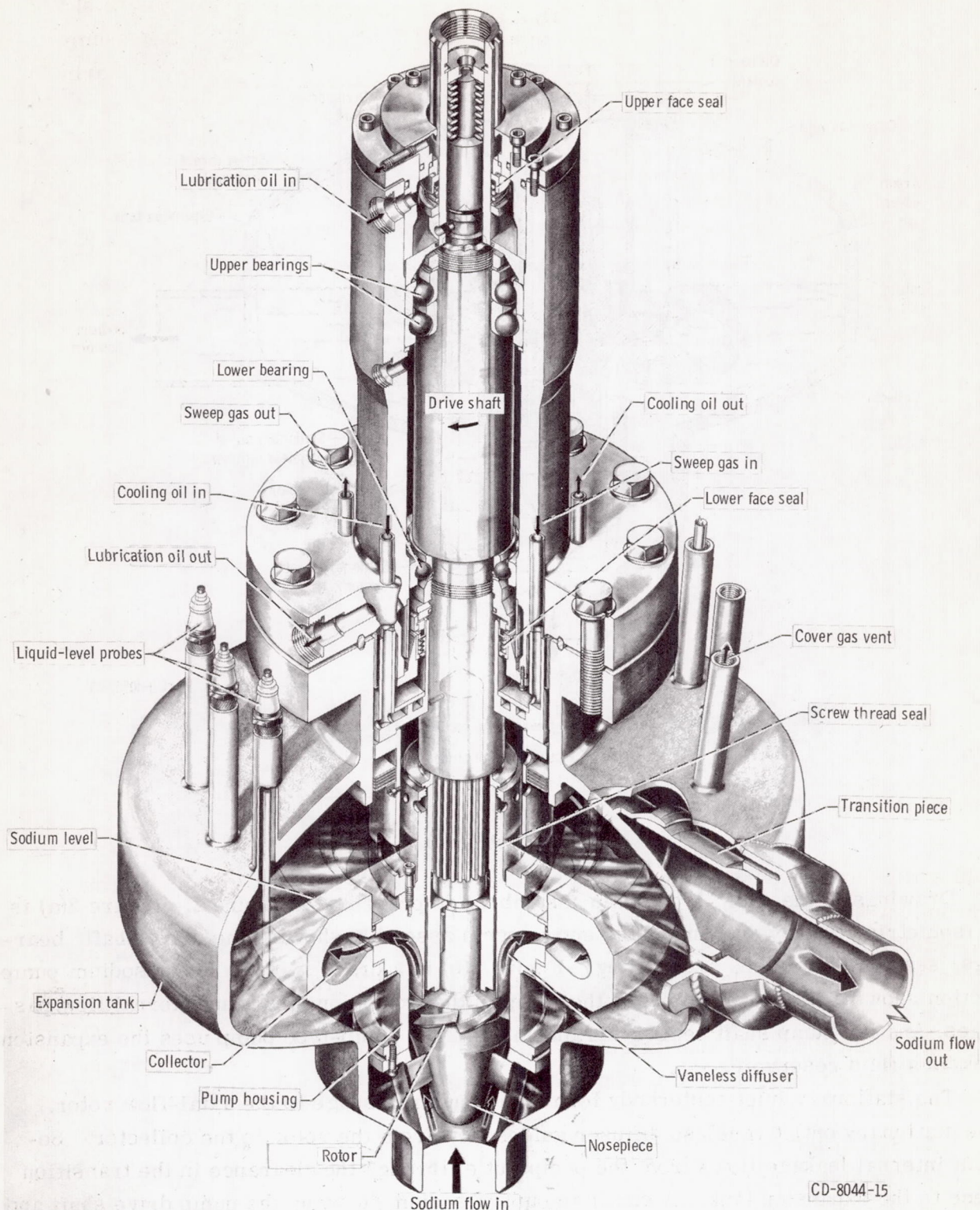
Rotor geometry:	
Tip diameter, in. (mm)	4.956 (126)
Hub-tip radius ratio	0.77
Number of blades	9
Blade-tip radial clearance, in. (mm)	0.033 (0.84)
Leading and trailing edge radii, in. (mm)	0.010 (0.254)
Tip geometry (double-circular-arc sections):	
Solidity, $\sigma_t$	1.00
Diffusion factor, $D_t$	0.40
Chord length, $c$ , in. (mm)	1.743 (44.3)
Ratio of maximum thickness to chord	0.06
Stagger angle with respect to axis, deg	76.5
Camber angle, deg	4.0
Incidence angle, $i_t$ , deg	2.8
Deviation angle, $\delta_t$ , deg	3.8
Inlet blade angle, $\kappa_{1,t}$ , deg	78.5
Hub geometry (double-circular-arc sections):	
Solidity, $\sigma_h$	1.30
Diffusion factor, $D_h$	0.60
Chord length, $c$ , in. (mm)	1.743 (44.3)
Ratio of maximum thickness to chord	0.08
Stagger angle with respect to axis, deg	70.5
Camber angle, deg	19.4
Incidence angle, $i_h$ , deg	-1.7
Deviation angle, $\delta_h$ , deg	8.9
Inlet blade angle, $\kappa_{1,h}$ , deg	81.0

316 stainless steel, three are 318 stainless steel, and three are Rene' 41 (a nickel-chromium-based superalloy).

Rotor design (ref. 1) is based on a blade element concept, with design calculations made across blade elements at a selected number of radial positions. These are then stacked to form a blade. Velocity diagrams were constructed by using the following design considerations and assumptions:

- (1) Constant inlet absolute axial fluid velocity at all blade radii
- (2) Constant energy addition at all blade radii
- (3) Simplified radial equilibrium
- (4) Constant blade efficiency at each section

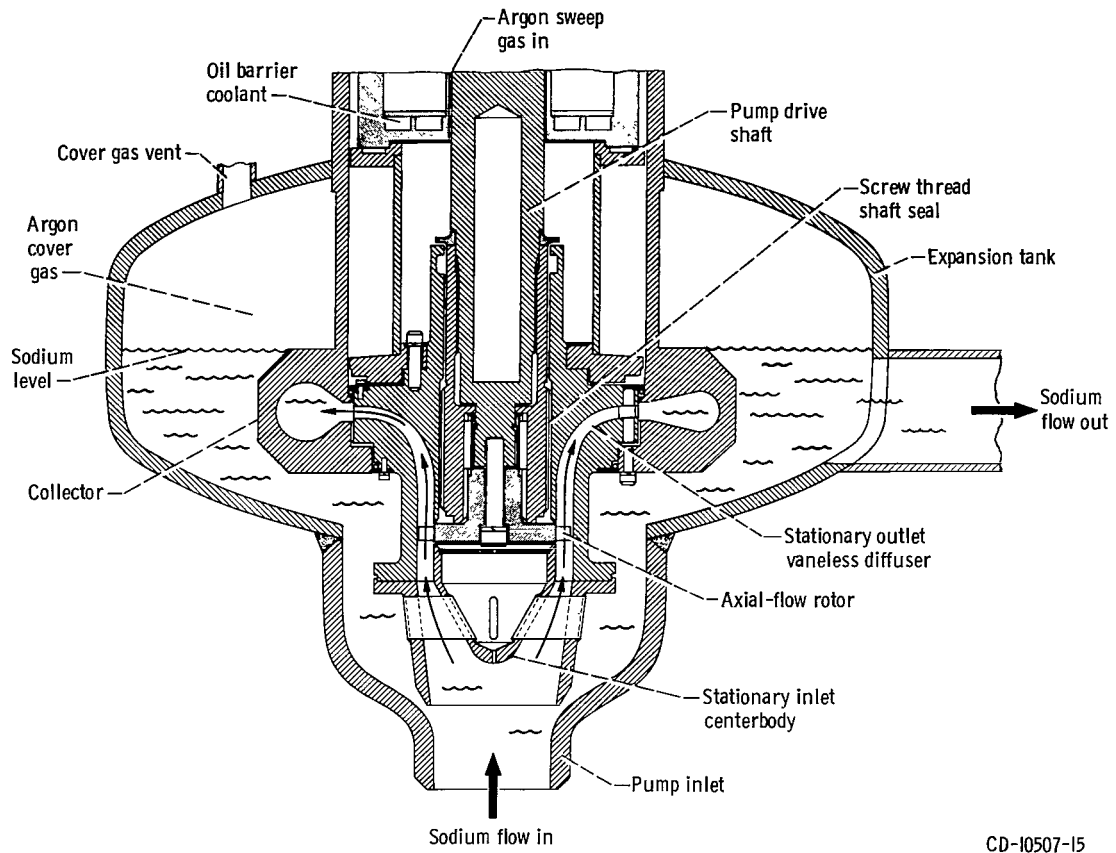
The basic design procedure follows that presented in reference 3 and utilizes design information from reference 4.



(a) Isometric cutaway (overall view).

Figure 2. - Sodium pump assembly.

CD-8044-15



(b) Lower pump section.

Figure 2. - Concluded.

## Pump Assembly

Drawings of the sump-type pump assembly are presented in figure 2. Figure 2(a) is an isometric cutaway drawing of the entire pump assembly showing the drive shaft, bearings, seals, lubrication, and cooling. Figure 2(b) is a drawing of the lower sodium pump section showing the arrangement of the pump in the expansion tank, the internal flow passages, and the pump shaft sealing arrangement. The sump-type pump uses the expansion tank as a fluid reservoir.

The stationary inlet centerbody forms an annular passage to the axial-flow rotor. The stationary outlet vaneless diffuser guides flow from the rotor to the collector. Sodium internal leakage flows from the pump outlet through the clearance in the transition piece to the expansion tank. A small amount of sodium flows up the pump drive shaft and through the triple-threaded screw-type shaft seal to the expansion tank. The pump shaft is mounted vertically and is supported by angular-contact oil-lubricated ball bearings.

Oil sealing is accomplished with rotating face seals. Argon gas flows around this lower face seal and down a close-clearance annular passage around the pump shaft and is vented from the expansion tank. This downflow of argon gas prevents sodium deposition on this lower face seal and on the cooler portions of the pump shaft.

## Test Facility

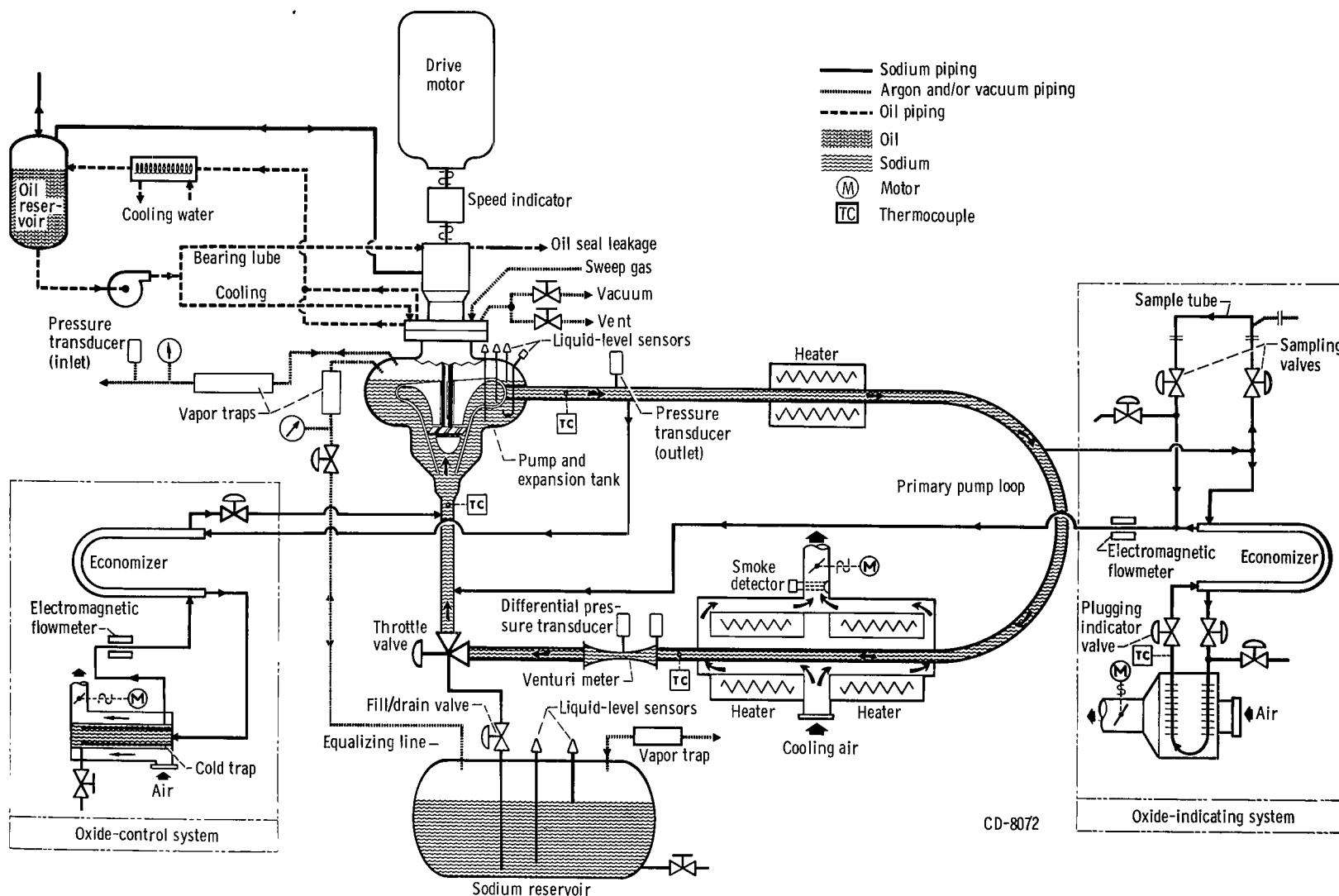
The alkali-metal pump test facility is capable of testing liquid-sodium pumps to temperatures of  $1500^{\circ}$  F (1089 K) and pressures to 150 psia ( $1.035 \times 10^6$  N/m<sup>2</sup> abs). A schematic diagram and an isometric drawing of the alkali metal pump test facility are presented as figure 3. The test facility comprises three sodium process systems: the primary sodium pump loop, the oxide control system, and the oxide indicating and sampling system. The primary sodium pump loop contains the pump and expansion tank, a venturi flowmeter, a throttle valve, electric heaters, and an air cooler. The oxide control system removes dissolved sodium oxide from the sodium test fluid, by cold trapping, in order to maintain the oxide weight concentration at 50 parts per million or less. The concentration is determined with the oxide indicating and sampling system. All sodium process piping is electrically heated with resistance-type heaters and is covered with high-temperature thermal insulation.

## Instrumentation

Major instrumentation considerations in alkali-metal systems are the high operating fluid temperature and the unique problems of plugging and corrosion associated with high oxygen content in the alkali metal. Instrumentation is provided to measure system fluid pressures, flows, temperatures, liquid level, and pump rotor speed. A description follows of the instrumentation used to determine these parameters.

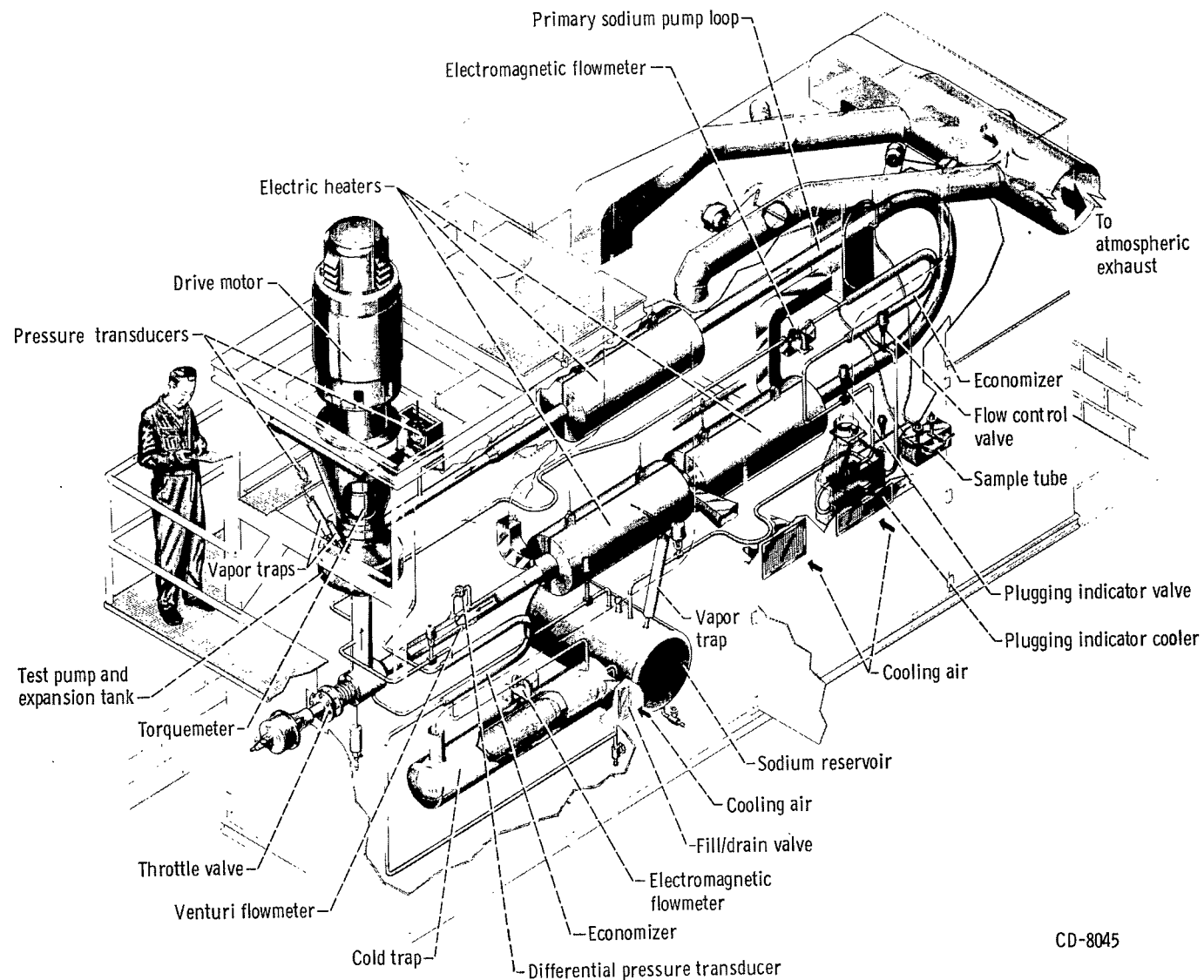
Pressure. - Pump inlet and outlet static pressures are sensed with unbonded wire strain-gage-type absolute pressure transducers. The inlet pressure transducer and a precision absolute pressure gage were used to measure the argon cover gas pressure in the expansion tank. The line from the tank to the transducer included a vapor trap. The outlet static pressure transducer is isolated thermally from the high-temperature sodium by inert argon gas in a vertical pressure line.

Flow. - Primary system sodium flow was determined by means of an air-calibrated venturi flowmeter with a throat diameter of 1.680 inches (4.26 cm) at room temperature. A volumetric differential pressure transducer was used to measure the static pressure drop from flowmeter inlet to throat. Electromagnetic flowmeters were used to measure



(a) Schematic drawing.

Figure 3. - Alkali-metal pump test facility.



CD-8045

(b) Overall isometric.

Figure 3. - Concluded.

oxide-control and oxide-indicating system flows, each of which was less than 1 percent of the research pump flow.

Temperature. - Thermocouples used to measure pump inlet, pump outlet, and venturi inlet temperatures were fabricated from calibrated Chromel-Alumel thermocouple wire and were installed in pipe wells located approximately at the system pipe centerline.

Liquid level. - Sodium liquid level in the expansion tank was sensed continuously by a resistance-type "J" probe.

Speed. - Pump speed was sensed with a magnetic pickup located on the pump shaft and was indicated on an electronic counter.

## Procedure

Noncavitating pump performance is obtained by varying the flow at constant rotative speed, fluid temperature, and net positive suction head (NPSH). Cavitating performance is obtained by reducing pump inlet pressure at constant rotative speed, fluid temperature, and flow until pump head rise decays approximately 30 percent. A 32-hour cavitation endurance test was conducted at a head-rise-coefficient ratio of approximately 0.96. During this endurance test the throttle valve was manually adjusted when necessary to maintain constant pump flow. Pump speed and inlet temperature were automatically controlled at a set point. The oxygen content of the sodium was maintained at or below 50 parts per million by weight.

Experimental data were reduced and corrected to account for

- (1) Instrument calibration
- (2) Thermal expansion of pump parts and of the venturi flowmeter
- (3) Variation of sodium fluid properties with temperature
- (4) Hydrostatic heads in the expansion tank and pressure transducer lines
- (5) Variation of venturi flowmeter coefficient of discharge with throat Reynolds number
- (6) Oxide-control and indicating system flows which bypass the venturi flowmeter

Overall pump performance is based on the measured static pressures in the expansion tank and the pump outlet line and is adjusted for the computed velocity and hydrostatic heads. Thus, pump total head rise accounts for the head losses in the pump inlet, the outlet diffuser, and the collector. Pump flow, which was used to calculate flow coefficient, is venturi flow plus oxide control and indicating system flow, but does not include internal leakage flow. Leakage was not measured but was estimated to vary from 3 to 10 percent of total flow over the pump operating range. Net positive suction head was calculated from the inlet total head minus the vapor head corresponding to the fluid inlet temperature.

The estimated experimental precision of pertinent test measurements and pump performance parameters at approximately design flow of 550 gallons per minute (0.0348 m<sup>3</sup>/sec) is presented in table II.

TABLE II. - EXPERIMENTAL PRECISION

[Design flow rate, Q, 550 gal/min (0.0348 m<sup>3</sup>/sec).]

Parameter	Precision
Fluid:	
Temperature, °F (K)	±10.0 (±5.6)
Static pressure, psi (N/m <sup>2</sup> ):	
Pump inlet, p <sub>1</sub>	±0.03 (±205)
Pump outlet, p <sub>2</sub>	±0.13 (±900)
Venturi differential	±0.19 (±1300)
Pump:	
Rotative speed, N, rpm	±2.0
Flow, Q, gal/min (m <sup>3</sup> /sec)	±7.0 (±4.4×10 <sup>-4</sup> )
Head rise, ΔH, ft (m)	±0.9 (±0.3)
Net positive suction head,	
H <sub>sv</sub> , ft (m)	±1.6 (±0.5)
Suction specific speed, S <sub>s</sub>	±525
Flow coefficient, φ	±0.004
Head-rise coefficient, ψ	±0.005

## RESULTS AND DISCUSSION

A 5-inch (127-mm) axial-flow rotor with three different blade materials was tested for 232 hours in liquid sodium at temperatures of 1000° and 1500° F (811 and 1089 K). Pump test results are presented in three sections: noncavitating performance, cavitating performance, and rotor cavitation damage.

### Noncavitating Performance

Pump noncavitating performance is presented in figure 4, which exhibits head-rise coefficient  $\psi$  as a function of flow coefficient  $\phi$ . Pump performance in liquid sodium is shown as a band of data for rotative speeds of 3500, 5000, and 7200 rpm for fluid temperatures of 1000° and 1500° F (811 and 1089 K). Analysis of the data indicates no systematic variation of noncavitating performance with either fluid temperature or rotative

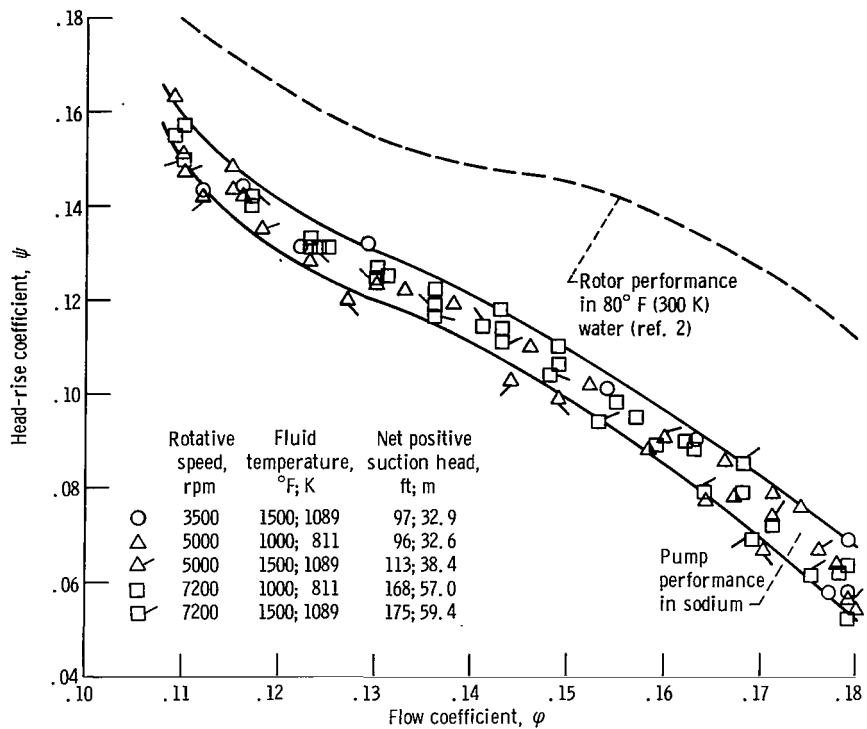


Figure 4. - Noncavitating performance of axial-flow pump in sodium and rotor in water.

speed. Pump noncavitating performance is virtually independent of fluid temperature over this range. The blade chord Reynolds number varied from  $2.5 \times 10^6$  to about  $8.0 \times 10^6$  over the range of operating conditions.

Also shown in figure 4 is the performance of a rotor of identical design (except for direction of rotation) which was tested in room-temperature water (ref. 2). The performance curve for the water rotor has an inflection near the middle of the flow range. A similar trend is noted in the data band for the sodium pump.

Rotor performance in water is based on pressure probe readings taken immediately upstream and downstream of the rotor. Sodium pump performance is overall pump performance and includes the pressure losses incurred in pump inlet, outlet diffuser, and collector. The unmeasured internal leakage flow in the sodium pump and a large rotor tip clearance necessitated by high-temperature operation also contribute to the difference in performance of the pump in sodium as compared to the rotor in water.

## Cavitating Performance

Pump cavitating performance was obtained at rotative speeds of 5000 and 7200 rpm and at liquid-sodium temperatures of 1000° and 1500° F (811 and 1089 K). Performance

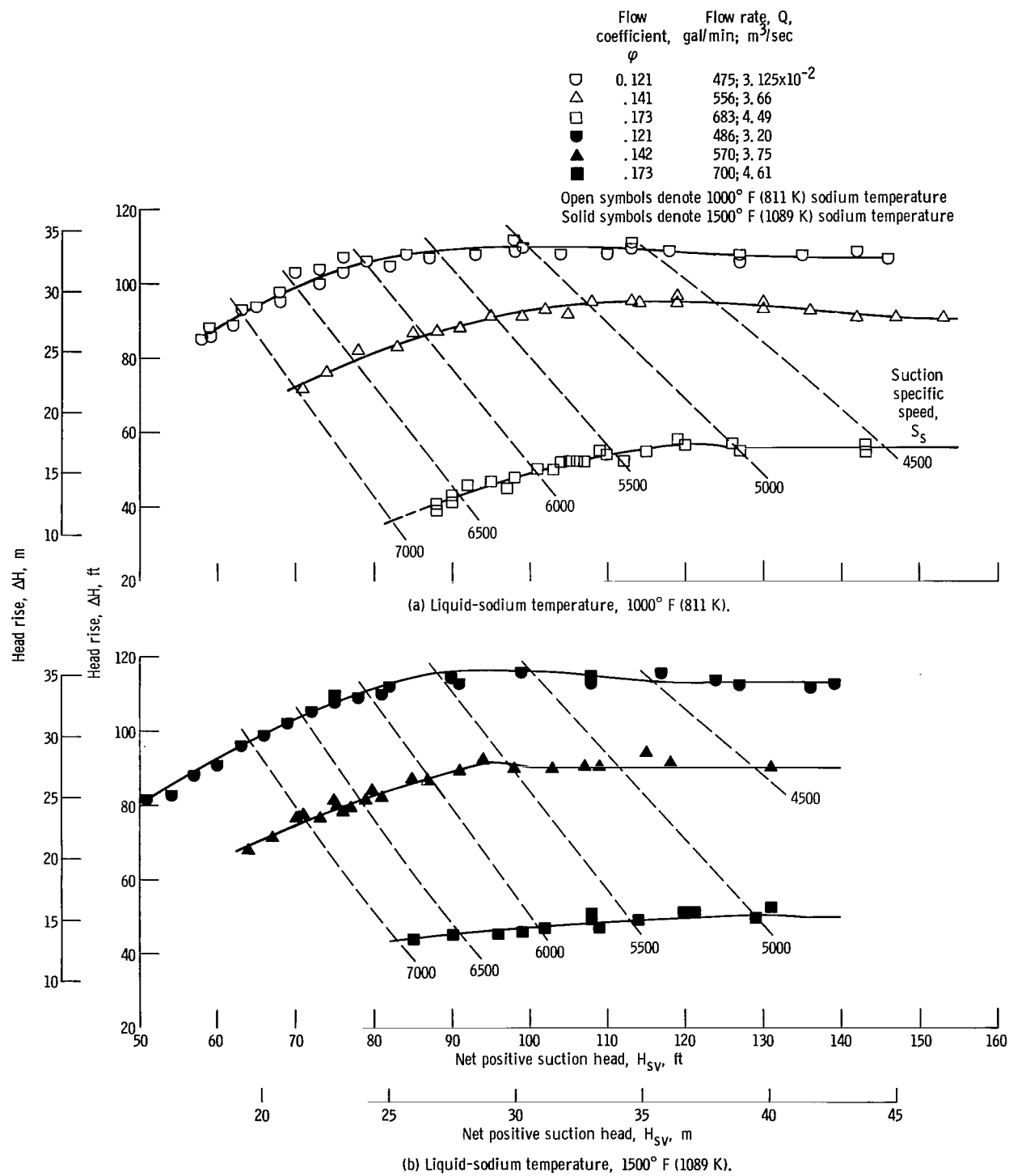


Figure 5. - Pump cavitating performance in sodium at 7200 rpm and three flow coefficients.

was evaluated at three different flow coefficients. Cavitation performance is presented in figures 5 and 6, where pump head rise  $\Delta H$  is shown as a function of net positive suction head  $H_{sv}$ . The superimposed dashed curves represent values of constant suction specific speed.

Pump cavitating performance at 7200 rpm is presented in figure 5 for  $1000^{\circ}\text{F}$  and  $1500^{\circ}\text{F}$  (811 and 1089 K) sodium for three nominal flow coefficients of 0.121, 0.142, and 0.173. For each temperature, initial pump head-rise dropoff occurs in the suction specific speed range of 5900 to 5100 over the flow coefficient range. This modest suction capability is attributed to the low blade-tip solidity of 1.0 and the high hub-tip radius ratio of 0.77. These values were dictated by the requirements of insertable blades and the system flow characteristics, respectively. In general, the head rise increases slightly before dropoff as the net positive suction head is reduced.

Pump cavitating performance at 5000 rpm is presented in figure 6. Performance at  $1500^{\circ}\text{F}$  (1089 K) is displayed at the two lower flow coefficients of 0.124 and 0.145. At  $1000^{\circ}\text{F}$  (811 K), performance at only the near-maximum flow coefficient of 0.169 was obtained because of pump shaft seal oil leakage at very low pump inlet pressures. Initial pump head-rise dropoff occurred in the same suction specific speed range ( $\sim 5500$ ) as at 7200 rpm. The same trend of increasing head rise before dropoff occurs with the 5000-rpm data as with the 7200-rpm data.

Due to the facility limitations during the 5000-rpm run, data were not obtained at the same flow coefficients at the two temperatures. And the effect of temperature could not

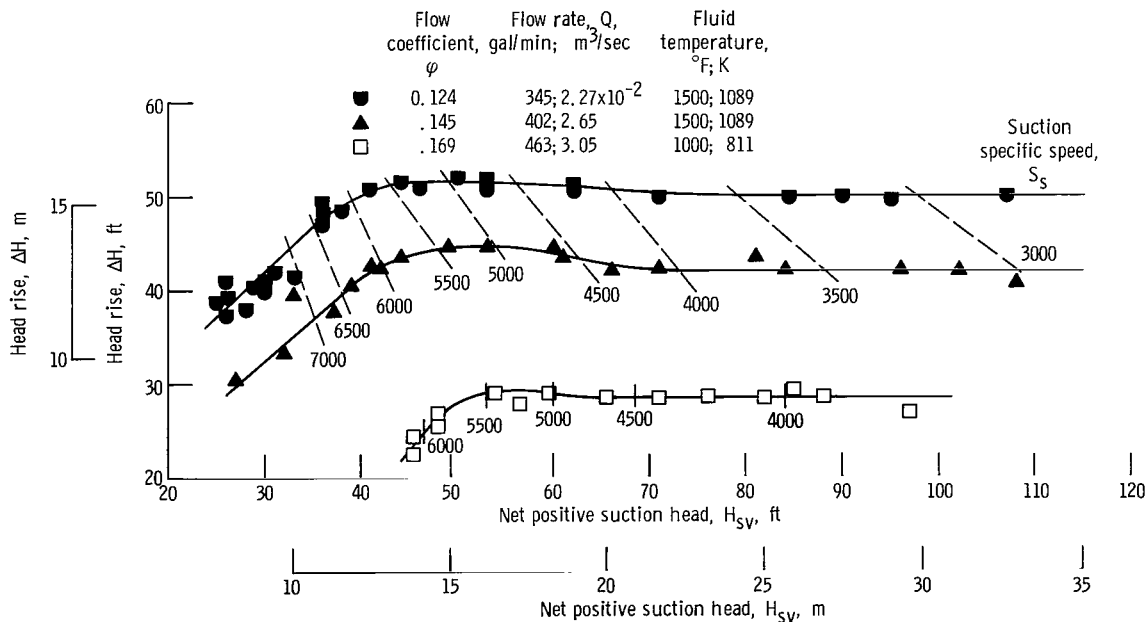


Figure 6. - Pump cavitating performance at 5000 rpm at two liquid-sodium temperatures and three flow coefficients.

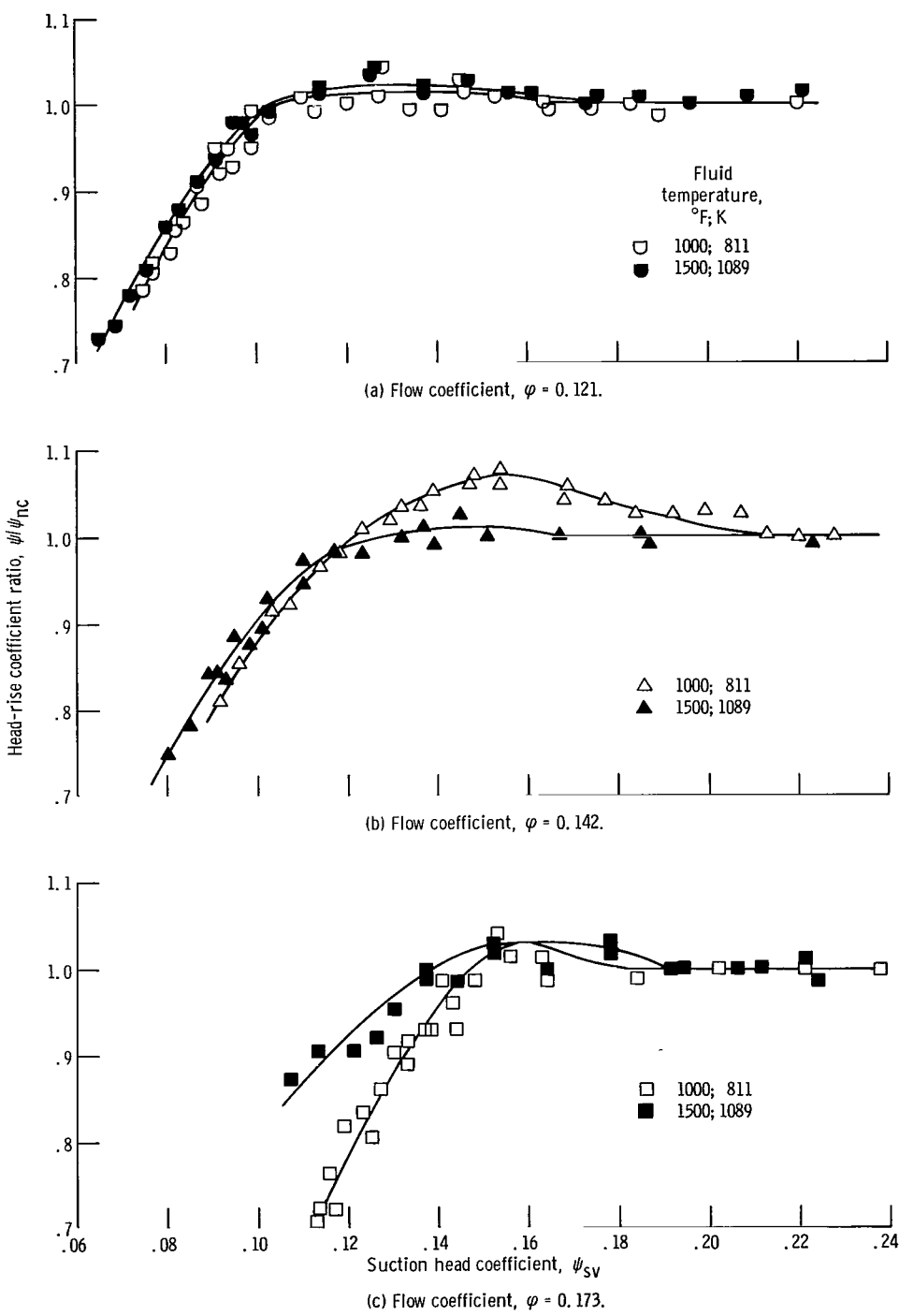


Figure 7. - Pump cavitating performance at 7200 rpm at two liquid-sodium temperatures.

be evaluated directly with the 5000-rpm data alone. However, the effect of temperature can be determined by presenting each cavitating curve in dimensionless parameters for both the 5000- and 7200-rpm data.

Therefore, cavitating performance of the axial-flow pump in normalized dimensionless parameters at 7200 rpm is presented in figure 7. Pump head-rise-coefficient ratio  $\psi/\psi_{nc}$  is presented as a function of suction head coefficient  $\psi_{sv}$ , at sodium temperatures of  $1000^{\circ}$  and  $1500^{\circ}$  F (811 and 1089 K) for each of the three nominal flow coefficients. Head-rise-coefficient ratio is a normalized form of pump head rise. The noncavitating head rise was obtained at a relatively high value of net positive suction head for each particular cavitation run. Suction head coefficient is a dimensionless form of net positive suction head. In general, these two parameters can be used to correlate cavitation performance data over a range of pump rotative speeds, flows, and, within limits, temperatures.

At all three flow coefficients, there is an effect of temperature on cavitating performance. The difference in the required suction head coefficient for the two temperatures at the same head-rise-coefficient ratio is a measure of the effect of fluid temperature on cavitation performance. For the nominal flow coefficients of 0.121 and 0.142 (figs. 7(a) and (b)), there is a slight reduction in the required suction head coefficient at  $1500^{\circ}$  F (1089 K) as compared to the lower temperature of  $1000^{\circ}$  F (811 K). The magnitude of this difference is within the experimental accuracy of the data, and only the trend should be noted. For the nominal flow coefficient of 0.173 (fig. 7(c)), the reduction in required suction head coefficient is quite significant and is a measure of the effect of fluid temperature on cavitation performance. For this rotor, the head rise increases above the noncavitating value ( $\psi/\psi_{nc} > 1.0$ ) just before dropoff as the net positive suction head is reduced. A significant increase in the head-rise-coefficient ratio to about 1.07 may be observed at a nominal flow coefficient of 0.142 for the  $1000^{\circ}$  F (811 K) sodium fluid temperature.

All of the cavitation performance obtained at 5000 rpm is presented in normalized nondimensional parameters in figure 8. These curves are analogous to those exhibited in figure 7 for 7200 rpm, except that curves at the same flow coefficient are not available for both temperatures. From figure 8, for the two curves at a temperature of  $1500^{\circ}$  F (1089 K) and at a given head-rise-coefficient ratio, suction head coefficient is greater for the curve of higher flow coefficient.

Pump cavitating performance in liquid sodium is summarized in figure 9. Required suction head coefficient is plotted as a function of flow coefficient for a head-rise-coefficient ratio of 0.9. The data points are from the faired curves of figures 7 and 8. Solid lines have been faired through the  $1000^{\circ}$  F (811 K) and  $1500^{\circ}$  F (1089 K) data. The figure indicates that required suction head coefficient increases approximately linearly with flow coefficient at a given temperature and head-rise-coefficient ratio. Within the

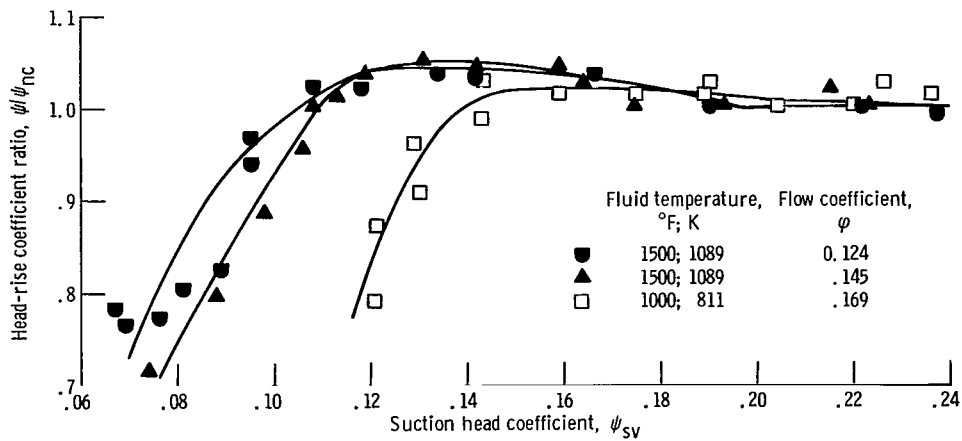


Figure 8. - Pump cavitating performance at 5000 rpm at two liquid-sodium temperatures and three flow coefficients.

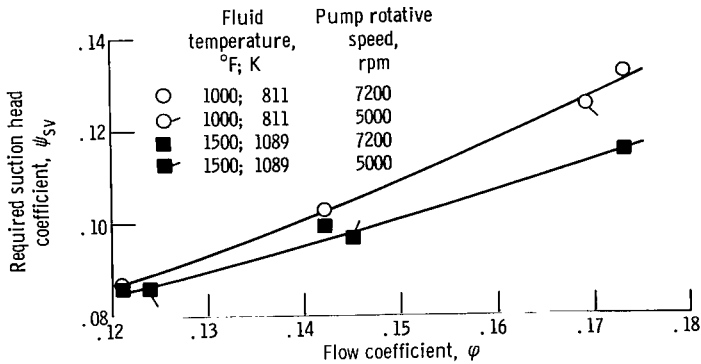


Figure 9. - Pump normalized cavitating performance at two rotative speeds and two liquid-sodium temperatures. Head-rise-coefficient ratio,  $\psi/\psi_{nc} = 0.9$ .

accuracy of the experimental measurements, suction head coefficient at a given temperature correlates cavitating performance at the rotative speeds of 5000 and 7200 rpm over the test flow coefficient range.

At a given head-rise-coefficient ratio and flow coefficient the difference between the 1000° and 1500° F (811 and 1089 K) values of required suction head coefficient is the effect of fluid temperature on cavitation performance. The data are presented in dimensionless parameters in figure 9 in order to determine required net positive suction head over the full experimental range of rotative speed and flow coefficient at either temperature. A temperature of 1000° F (811 K) was selected as roughly the highest convenient temperature at which there is no change in cavitation performance from that at a lower temperature. Calculations based on reference 5 indicate that increasing the temperature of sodium to 1000° F (811 K) would have no measurable effect on cavitation per-

formance, whereas a slight reduction in required net positive suction head would occur at  $1500^{\circ}$  F (1089 K).

At the lower flow coefficients, the difference in required suction head coefficient is very slight. The data indicate that the effect of fluid temperature on cavitation performance increases with increasing flow coefficient, increasing rotative speed, and decreasing ratio. Similar trends for the effect of fluid temperature on cavitation performance were obtained for a similar rotor tested in water at temperatures to  $250^{\circ}$  F (394 K) as reported in reference 2. At a flow coefficient of 0.173, the indicated suction head coefficient is about 0.132 for  $1000^{\circ}$  F (811 K) sodium and 0.116 for  $1500^{\circ}$  F (1089 K) sodium. For a rotative speed of 7200 rpm, this difference in suction head coefficient of 0.016 corresponds to about 13 feet (4 m) at the highest flow coefficient of 0.173. However, the actual magnitude of the improvement may have been affected by the differences in the noncavitating head rise and/or internal leakage flows at the two temperatures.

### Rotor Cavitation Damage

After the cavitation performance data were taken, a 32-hour cavitation test was conducted to evaluate qualitatively the resistance of the three blade materials to cavitation damage. The pump was operated at 7200 rpm in  $1500^{\circ}$  F (1089 K) liquid sodium at a near-design flow coefficient of 0.142 and a suction specific speed of about 6100. This resulted in a head-rise-coefficient ratio of about 0.96. The blades are manufactured from 316 stainless steel, 318 stainless steel, and Rene' 41.

The rotor sustained localized suction surface cavitation damage near the blade-tip leading edges. This damage is indicated in figure 10, which is a front view of the rotor. Each blade sustained damage in approximately this same location, and the general shapes of the damaged area of each blade are similar. A closeup view of the damaged area on each of the nine blades is shown in figure 11. The Rene' 41 blades sustained the least amount of damage, and the 316 stainless-steel blades sustained the most damage.

There is a marked blade-to-blade variation in the amount of damage. The three most severely damaged blades of each material are mounted in adjacent slots in the rotor hub (figs. 11(a) to (c)). The three blades of each material with the least damage are also mounted in adjacent slots (figs. (11(f) to (h))). These observations suggest a circumferential variation in flow conditions serious enough to generate a variance in damage among blades of the same material. These variations could be due to flow deviations in the rotor passages resulting from circumferential variations in tip clearance, variations in blade placement in the hub, thermal gradients, shaft runout, or shaft eccentricity in the casing.

The cavitation damage patterns observed in this rotor were attributed to blade-tip leading edge cavitation based on the visual and photographic observations of a virtually identical rotor tested in water (ref. 2). The damage patterns sustained by the rotor in

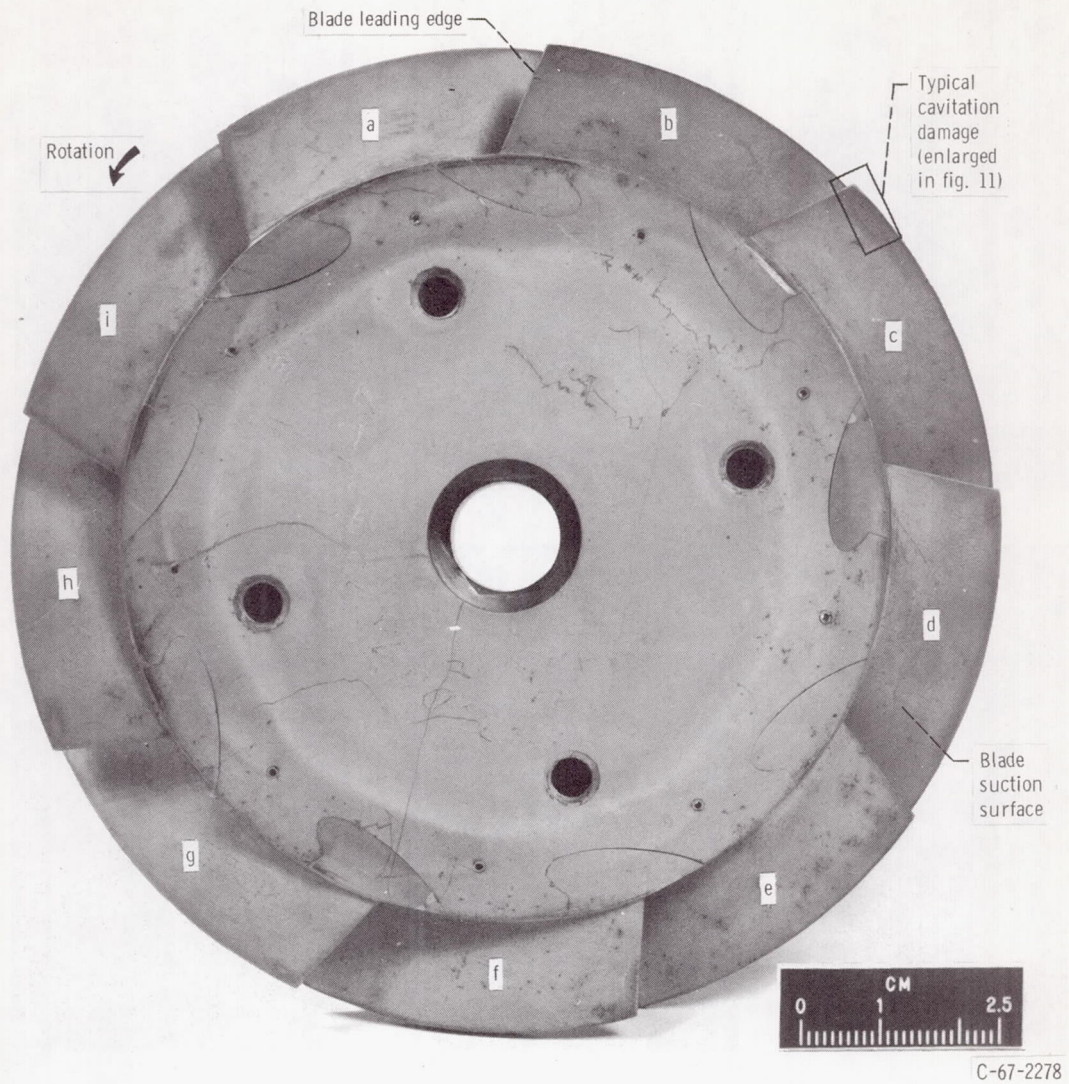


Figure 10. - Suction surface cavitation damage to pump rotor. Letters at each blade correspond with figure letters in figure 11.

water were similar to those sustained by the rotor in liquid sodium in this investigation. A comparison of figure 21 from reference 2 with figure 11 in this report will indicate this similarity.

In general, cavitation damage sustained by this rotor was more severe than that sustained by a virtually identical rotor tested in liquid sodium at 3450 rpm for 200 hours at otherwise similar operating conditions, including the same suction specific speed (ref. 1). The ranking of the three blade materials and the shape and location of the damaged areas were similar. The difference between the two tests was the rotative speed at which the two rotors were operated. As noted earlier, the present rotor was operated at 7200 rpm and the referenced rotor was run at 3450 rpm during the corresponding cavitation endur-

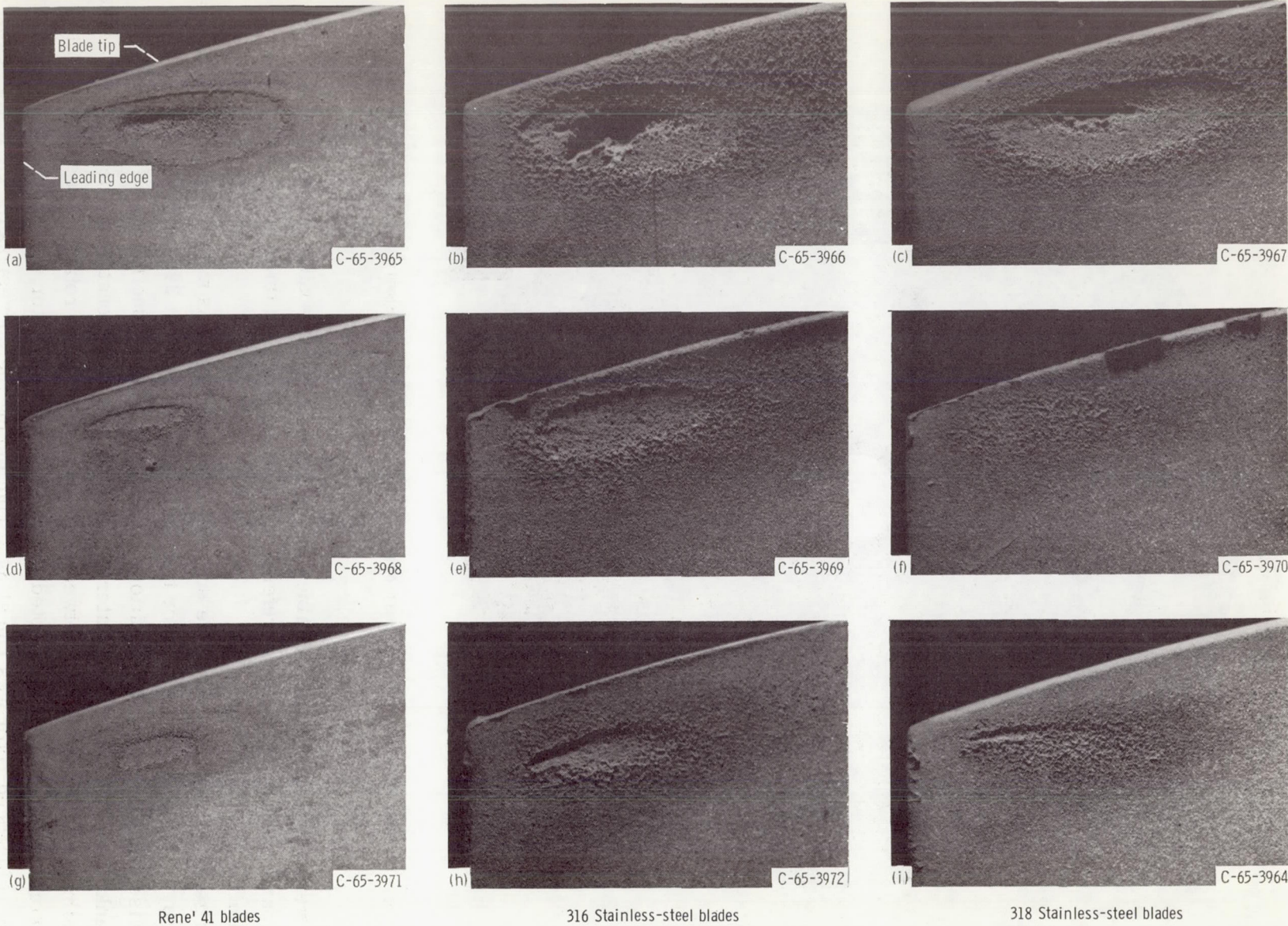


Figure 11. - Rotor blade suction surface damage sustained by each blade near blade-tip leading edge. Blades are pictured in the order in which they are installed on the rotor hub. Figure letters correspond with blade letter identification in figure 10.

ance tests. Apparently, the higher rotative speed with its resultant higher fluid velocities generates cavitation damage at a much faster rate, even though the suction specific speed during the two tests was about the same.

## SUMMARY OF RESULTS

A 5-inch (127-mm) axial-flow rotor with three different blade materials was tested for 232 hours in liquid sodium at temperatures of  $1000^{\circ}$  and  $1500^{\circ}$  F (811 and 1089 K). After obtaining noncavitating and cavitating performance, a 32-hour cavitation test was conducted in  $1500^{\circ}$  F (1089 K) sodium at 7200 rpm and at a suction specific speed of about 6100. Damage results are compared to those of reference 1. The following principal results were obtained:

1. Pump cavitating performance in liquid sodium is virtually independent of fluid temperature over the range from  $1000^{\circ}$  to  $1500^{\circ}$  F (811 to 1089 K). An inflection of the head-flow characteristic curve occurs near the design flow coefficient.
2. Required net positive suction head at  $1500^{\circ}$  F (1089 K) is less than that at  $1000^{\circ}$  F (811 K) for similar operating conditions. This effect of fluid temperature on cavitation performance increases with increasing flow coefficient, decreasing head-rise-coefficient ratio, and increasing rotative speed. Similar trends for the effect of fluid temperature on cavitation performance were obtained for a similar rotor in water at temperatures to  $250^{\circ}$  F (394 K), as reported in reference 2.
3. Experimental values of the effect of fluid temperature on cavitation performance in  $1500^{\circ}$  F (1089 K) sodium were slight at the low flow coefficient, but caused a decrease of about 13 feet (4 m) in the required net positive suction head at 7200 rpm and at the highest flow coefficient of 0.173.
4. The rotor blades sustained severe localized suction surface cavitation damage near the blade-tip leading edges. The Rene' 41 blades were the most resistant to this damage, with 318 stainless steel next, and 316 stainless steel rated the least resistant. There is a marked circumferential variation in the amount of damage on blades of the same material, which may be due to circumferential variations in flow or geometry.
5. Cavitation damage sustained by this rotor was more severe than that sustained by a similar rotor tested in  $1500^{\circ}$  F (1089 K) liquid sodium for 200 hours at 3450 rpm but at the same suction specific speed (ref. 1). Thus, the intensity of cavitation damage increases significantly with rotative speed at constant suction specific speed.

Lewis Research Center,  
National Aeronautics and Space Administration,  
Cleveland, Ohio, July 2, 1969,  
720-03.

## APPENDIX - SYMBOLS

c	blade chord length, ft (m)
D	blade diffusion factor, $1 - \frac{V'_2}{V'_1} + \frac{V'_{2,\theta} - V'_{1,\theta}}{2\sigma V'_1}$
g	gravitational constant, $32.17 \text{ ft/sec}^2$ ( $9.83 \text{ m/sec}^2$ )
H	total head, ft (m)
$\Delta H$	pump total head rise, $H_2 - H_1$ , ft (m)
$H_{sv}$	net positive suction head, $H_1 - h_v$ , ft (m)
h	static head, ft (m)
i	incidence angle, angle between direction of inlet flow relative to rotor and tangent to blade mean camber line at leading edge, $\beta'_1 - \kappa_1$ , deg
N	rotative speed, rpm
p	static pressure, psia ( $\text{N/m}^2$ abs)
Q	flow rate, gal/min ( $\text{m}^3/\text{sec}$ )
$S_s$	suction specific speed, $N\sqrt{Q_p}/(H_{sv})^{0.75}$
s	blade tangential spacing, ft (m)
U	rotor tangential velocity, ft/sec (m/sec)
V	fluid velocity, ft/sec (m/sec)
$\beta'$	flow angle, angle between direction of flow relative to rotor and axial direction, deg
$\delta$	deviation angle, angle between outlet flow direction relative to rotor and tangent to blade mean camber line at trailing edge, $\beta'_2 - \kappa_2$ , deg
$\kappa$	blade angle, angle between tangent to blade mean camber line at leading or trailing edge and axial direction, deg
$\sigma$	blade solidity, c/s
$\phi$	flow coefficient, $V_z, 1/U_t$
$\psi$	head-rise coefficient, $g\Delta H/U_t^2$
$\psi_{sv}$	suction head coefficient, $gH_{sv}/U_t^2$

**Subscripts:**

h hub  
nc noncavitating  
p pump  
t tip  
v vapor  
z axial direction  
 $\theta$  tangential direction  
1 pump inlet  
2 pump outlet

**Superscript:**

' relative to rotor

## REFERENCES

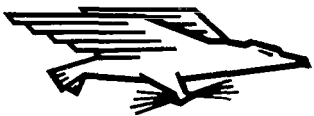
1. Reemsnyder, Dean C.; Cunnan, Walter S.; and Weigel, Carl: Performance and Cavitation Damage of an Axial-Flow Pump in 1500° F (1089 K) Liquid Sodium. NASA TN D-5138, 1969.
2. Cunnan, Walter S.; Kovich, George; and Reemsnyder, Dean C.: Effect of Fluid Temperature on the Cavitation Performance of a High Hub-Tip Ratio Axial Flow Pump in Water to 250° F (394 K). NASA TN D-5318, 1969.
3. Crouse, James E.; Montgomery, John C.; and Soltis, Richard F.: Investigation of the Performance of an Axial-Flow-Pump Stage Designed by the Blade-Element Theory-Design and Overall Performance. NASA TN D-591, 1961.
4. Johnsen, Irving A.; and Bullock, Robert O., eds.: Aerodynamic Design of Axial-Flow Compressors. NASA SP-36, 1965.
5. Ruggeri, Robert S.; and Moore, Royce D.: Method for Prediction of Pump Cavitation Performance for Various Liquids, Liquid Temperatures, and Rotative Speeds. NASA TN D-5292, 1969.

NATIONAL AERONAUTICS AND SPACE ADMINISTRATION

WASHINGTON, D. C. 20546

OFFICIAL BUSINESS

FIRST CLASS MAIL



POSTAGE AND FEES PAID  
NATIONAL AERONAUTICS AND  
SPACE ADMINISTRATION

06U 001 40 51 3DS 69273 00903  
AIR FORCE WEAPONS LABORATORY/WLIL/  
KIRTLAND AIR FORCE BASE, NEW MEXICO 87111

ATT: E. LOU BOWMAN, CHIEF, TECH. LIBRARY

POSTMASTER: If Undeliverable (Section 158  
Postal Manual) Do Not Return

*"The aeronautical and space activities of the United States shall be conducted so as to contribute . . . to the expansion of human knowledge of phenomena in the atmosphere and space. The Administration shall provide for the widest practicable and appropriate dissemination of information concerning its activities and the results thereof."*

— NATIONAL AERONAUTICS AND SPACE ACT OF 1958

## NASA SCIENTIFIC AND TECHNICAL PUBLICATIONS

**TECHNICAL REPORTS:** Scientific and technical information considered important, complete, and a lasting contribution to existing knowledge.

**TECHNICAL NOTES:** Information less broad in scope but nevertheless of importance as a contribution to existing knowledge.

**TECHNICAL MEMORANDUMS:** Information receiving limited distribution because of preliminary data, security classification, or other reasons.

**CONTRACTOR REPORTS:** Scientific and technical information generated under a NASA contract or grant and considered an important contribution to existing knowledge.

**TECHNICAL TRANSLATIONS:** Information published in a foreign language considered to merit NASA distribution in English.

**SPECIAL PUBLICATIONS:** Information derived from or of value to NASA activities. Publications include conference proceedings, monographs, data compilations, handbooks, sourcebooks, and special bibliographies.

**TECHNOLOGY UTILIZATION PUBLICATIONS:** Information on technology used by NASA that may be of particular interest in commercial and other non-aerospace applications. Publications include Tech Briefs, Technology Utilization Reports and Notes, and Technology Surveys.

*Details on the availability of these publications may be obtained from:*

**SCIENTIFIC AND TECHNICAL INFORMATION DIVISION**

**NATIONAL AERONAUTICS AND SPACE ADMINISTRATION**

Washington, D.C. 20546